AD NUMBER

AD489933

LIMITATION CHANGES

TO:

Approved for public release; distribution is unlimited.

FROM:

Distribution authorized to U.S. Gov't. agencies and their contractors; Critical Technology; FEB 1964. Other requests shall be referred to U.S. Army Research Office-Durham, Box CM, Duke Station, Durham, NJ 27706. This document contains export-controlled technical data.

AUTHORITY

USAROD ltr, 4 Aug 1971

Interim Technical Report

PLASTER OF PARIS AS A STATIC & DYNAMIC MODEL TESTING MATERIAL

by

George K. Coffin and Sudhir Kumar

February 1964

U. S. Army Research Office-Durham

Box CM, Duke Station

Durham, N. C.

INTERIM TECHNICAL REPORT

PLASTER OF PARIS AS A STATIC & DYNAMIC MODEL TESTING MATERIAL

by

George K. Coffin and Sudhir Kumar

February 1964

U. S. ARMY RESEARCH OFFICE - DURHAM

Box CM, Duke Station

Durham, N. C.

TABLE OF CONTENTS

LIST OF FIGURES AND TABLES

Chapter I

INTRODUCTION

1.1 General Comments

Plaster of Paris and highgrade pottery plaster have been used for over thirty years as a modelling material. In the field of experimental study of elastic stresses with models, plaster has been a desirable material because of its ease of casting into any desired shape, its linear stress-strain relation up to fracture, its low modulus of elasticity and fracture strength, and its small grain size. Its linear stress-strain characteristics up to fracture and high compressive strength in comparison to its tensile strength have made it a desirable material to be used in the brittle-model method of stress analysis. When plaster models are used for the estimation of stress in a certain elastic structure, it is usually termed as the plaster-model method.

1.2 Plaster Model Method

This method may be explained as follows: A model of irregular shape in which the stress is to be found is made of plaster and a calibration specimen of the same material is made of a simple shape. The calibration specimen is tested to failure for determining its ultimate tensile strength, and the irregular-shaped model is also loaded to failure and the load recorded. The stress in the region of the model where fracture begins is approximately equal to the ultimate tensile strength of the calibration specimen. The stress at the point of fracture in the model being known for a certain load, its value corresponding to other loads can be easily calculated because of the linear relationship of stress with load. For example: if a model is made of plaster having an ultimate tensile strength of 600 psi and a load of 200 lbs. is required to cause a fracture at the weakest point, the stress-load relation at the weakest point in the model and a gecmetrically identical brittle prototype is 3 psi per lb. of load.

A load of 5,000 lbs. on the prototype will produce a stress of 15,000 psi at the weakest point and if the prototype material has an ultimate tensile strength of 30,000 psi, its approximate load capacity is 10,000 lbs.

1.3 Previous Studies of Plaster as a Modelling Material

The plaster-model method was used initially in the 1920's and 30's for the investigation of strengths and stress concentrations at fillets, holes, and keyways by R.E. Peterson[1], Seeley and Dolan[3], and Trinks and Hitchcock[4]. Determination of strengths and points of structural weakness in curved beams with a variety of cross sections[2] and slabs subjected to concentrated loads and different support conditions[5] were also made using the plaster-model method.

The previous investigations were concerned with the prediction of tensile stresses at the point of weakness in structural and machine members, but recently, plaster was used as a modelling material for non-fracture elastic deflection type tests[6] carried out on a rectangular plate simply supported on its two short sides and stiffened by ribs on the two long edges.

This was equivalent to a highway bridge with two main girders and a monolithic slab. Plaster was used because it has a desirably low modulus of elasticity which enables one to obtain measurable deformations with relatively small loads. Also it can be cast and machined into the desired shape with ease.

Most of the investigations using the plaster-model method for determination of stress were made before 1940. The use of this method seems to have become almost unknown since then. Its neglect in stress analysis, in the author's opinion, was due to several factors. During World War II, stress analysts developed several accurate and fast strain measuring methods and gages. The biggest impact was made by the invention of the SR-4 type wire resistance strain gage. Other strain gages, both optical as well as mechanical, also offered a means of accurate and simple measurement of strain. The photoelastic method of stress analysis and more recently, strain gages like "Photostress" have been greatly advanced by the development of new and better plastics. The brittle coatings like "Stresscoat" have also presented a new stress measurement technique.

These advances in stress and strain measurement can fulfill most of the requirements of the design engineer for experimental stress analysis of a given structure. However, in narrow regions which are hard to reach by finite area gages, that is internal notches, grooves and fillets within a three dimensional design shape like a pump housing, determination of stress concentrations is still extremely difficult. It is in these situations that the plaster-model method still offers an easy and practical answer. It becomes very simple, especially for the elastic stress analysis of castings for which molds are already prepared. These very molds can be used for making plaster models, thereby, reducing a considerable amount of work.

Not only can plaster be used effectively as a modelling material for static tests, but it has been found to be useful as a dynamic testing material also. The use of plaster of Paris for dynamic studies was suggested in 1957 by Kumar and Davids[7]. They indicated that plaster of Paris would be a suitable material for a study of the scabbing phenomenon as a large number of scabs (as many as five) could be produced from a bar when a strong pressure pulse was generated at one end either by impact or explosion.

There are several other reasons which make this material suitable for dynamic testing. They are:

1. High ratio of compressive to tensile strength.
2. Low tensile strength which requires only a small magnitude of force to produce scabs.
3. A linear stress-strain relation both in compression and tension.
4. Relative ease of handling and casting.

Recently studies have been made by Kumar[8], Jones[9], and Leu[10], on scabbing in bars and plates using plaster of Paris as a modelling material.

The physical and mechanical properties of plaster are dependent on: the proportion of water used in mixing; blending time; mixing method; curing conditions; and age of the specimen. The proportion of water used in mixing and the blending time have the greatest effect upon the ultimate compressive strength of the case. The ultimate compressive strength and density [11], ultimate tensile strength, and elastic modulus [13] increase with decreasing proportions of water.

1.4 Reasons for the Present Study

The usefulness of plaster as a dynamic testing material, for studies like those of scabbing, is directly related to its compressive to tensile strength ratio; the higher this value, the better. Because of this it was felt that a study should be made to determine under what conditions this ratio is maximum. The mix used by some investigators [9,10] has been 65 parts water per 100 parts plaster by weight without a definite blending time. When the mix with the greatest compressive to tensile strength ratio is obtained, optimum blending time should be determined. In previous scabbing experiments [9,10] using plaster of Paris models, the dynamic tensile strength was taken to be twice the static value; so a study should be made to determine this value. Also the opportunity would be on hand to introduce a schedule for procuring a relatively consistent homogeneous mix, free from entrapped air. Because of these reasons, this study of plaster of Paris as a static and dynamic model testing material was undertaken.

1.5 Comments On The Plaster Used

The properties of plaster of Paris presented in this paper are representative of one 90 lb. shipment of plaster produced by the United States Gypsum Company and sold under the brand name of "Red Top". These properties may vary somewhat for products of different manufacturers and also for different shipments of the same manufacturer. Therefore, properties of the plaster determined in this thesis should be taken as approximate for other plasters. For accurate work with plaster, it will be desirable to conduct tests to determine the individual properties of the particular batch used. The methods of testing as developed in this thesis may be used.

Chapter II

PREPARATION OF THE SPECIMENS

As stated in section 1.4 the material used is plaster of Paris produced by the United States Gypsum Company and sold under the brand name of "Red Top".

2.1 Schedule

Several steps were taken to obtain consistent results from the tests, such as: drying of plaster in an 80°F oven for at least 24 hrs. before use; distillation of mixing water; thorough cleaning of mixing apparatus after each use; maintaining a relatively constant batch size; and covering the mixing container with a wet cloth to prevent evaporation during blending. After weighing desired amounts of plaster and water, the plaster was poured into the water.

Time elapsed between putting the plaster into water and beginning of stirring was recorded as the blending time.

Upon completion of the desired blending time, a vacuum, vibration, and slow stirring was applied to the mix for removal of entrapped air. Vacuum was applied after blending to eliminate a mixing action caused by rising air bubbles (Fig. 1) . When the mix became smooth and apparently free from entrapped air, the vacuum and stirring was terminated and one end of a lightly oiled mold, made of plastic tubing, was placed into the mix. A slight vacuum was applied to the other end, thereby, causing the tube to be filled with the mix. Vibration was continued during drawing to assure a steady flow of mix into the mold (Fig. 1).

It was found that this method of casting produced specimens with fewer air holes than the conventional method of pouring the mix in the mold. Also, it was not necessary to split the molds in the longitudinal direction to facilitate removal of the specimens because they are easily removed from the mold at the time in which the plaster gives off heat. Removal is accomplished by tapping one end of the mold on a solid object and then pushing the specimen out with a plunger.

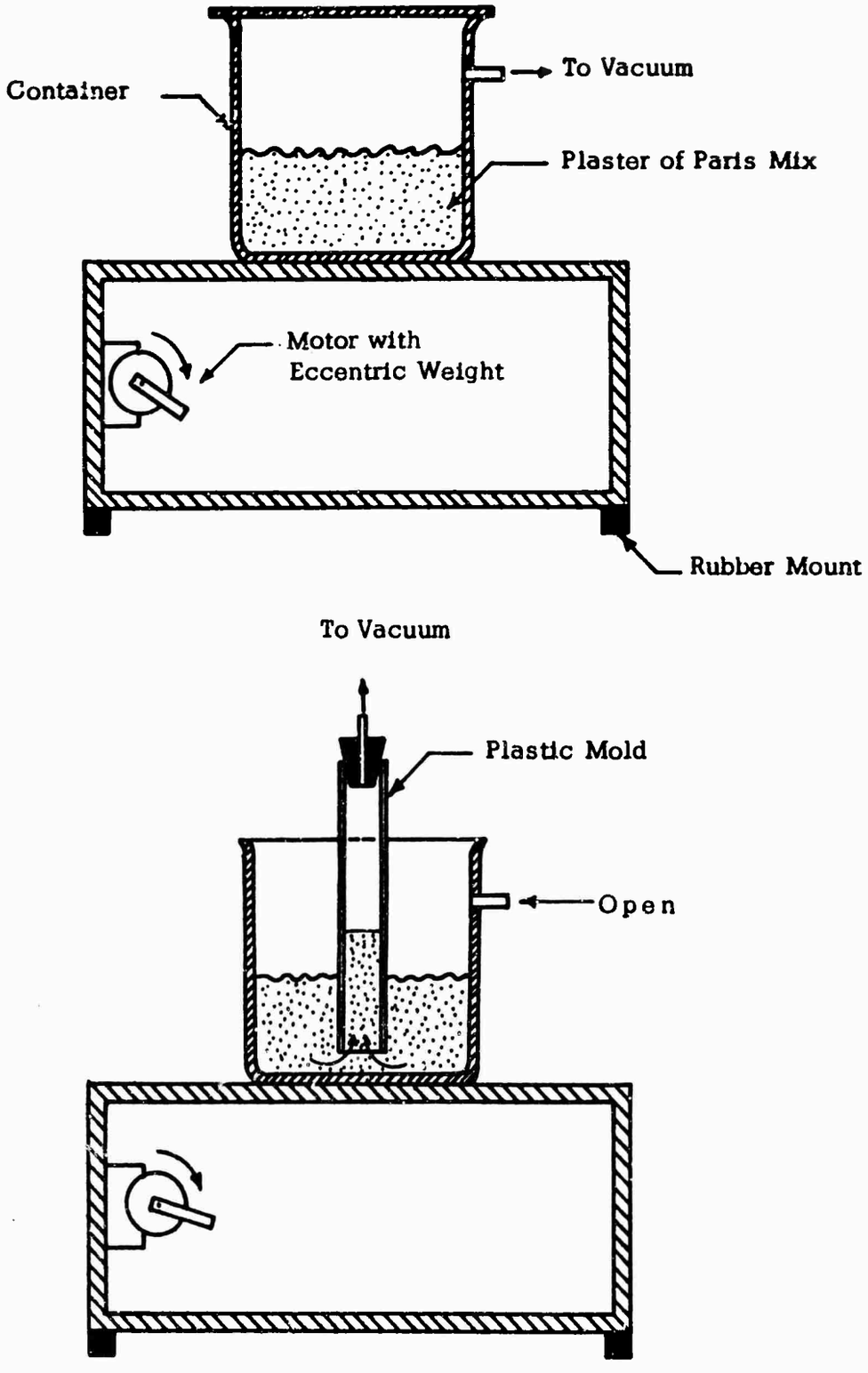

Fig. 1. Mixing and Casting of Plaster of Paris Specimens.

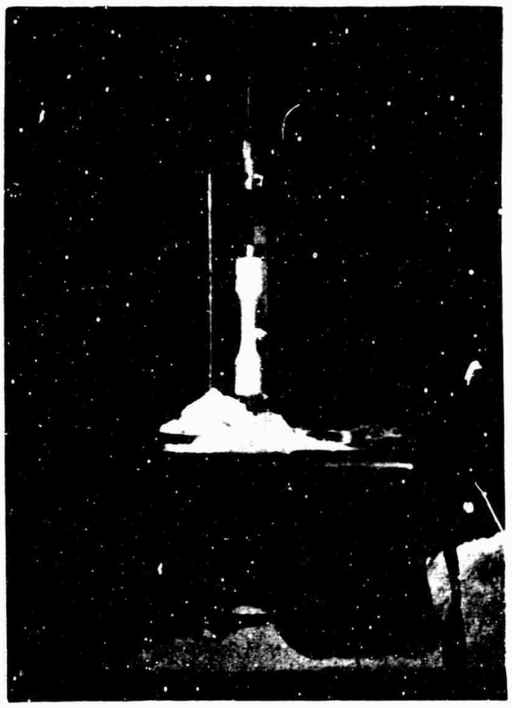

Fig. 2. Machining of Tension Specimens.

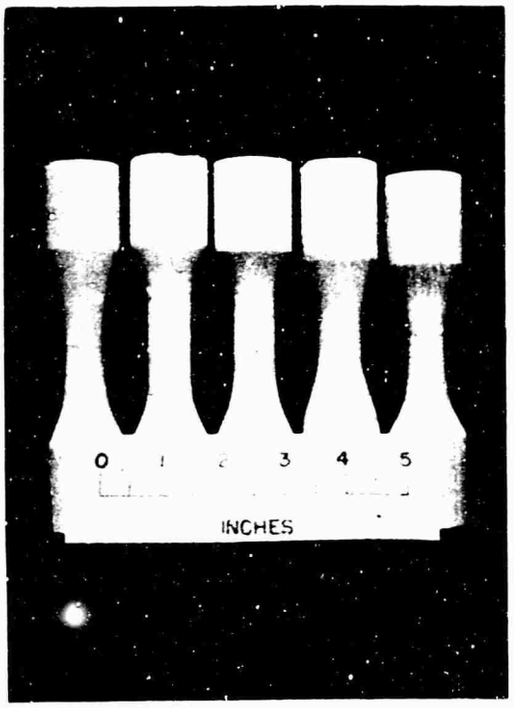

Fig. 3. Tension Specimens.

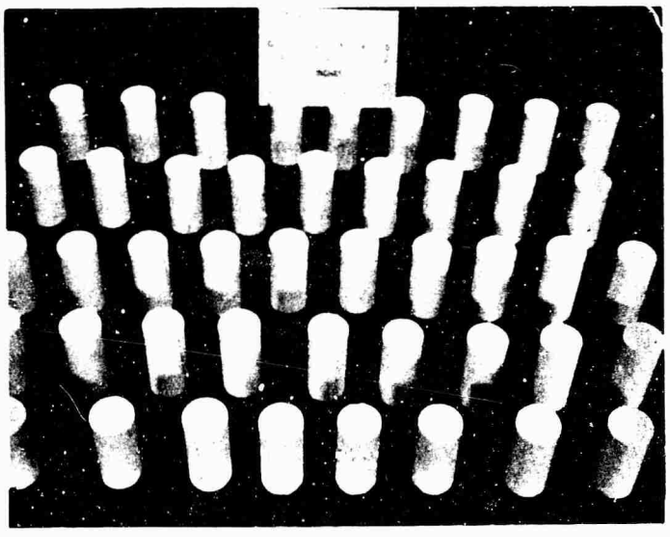

Fig. 4. Compression Specimens.

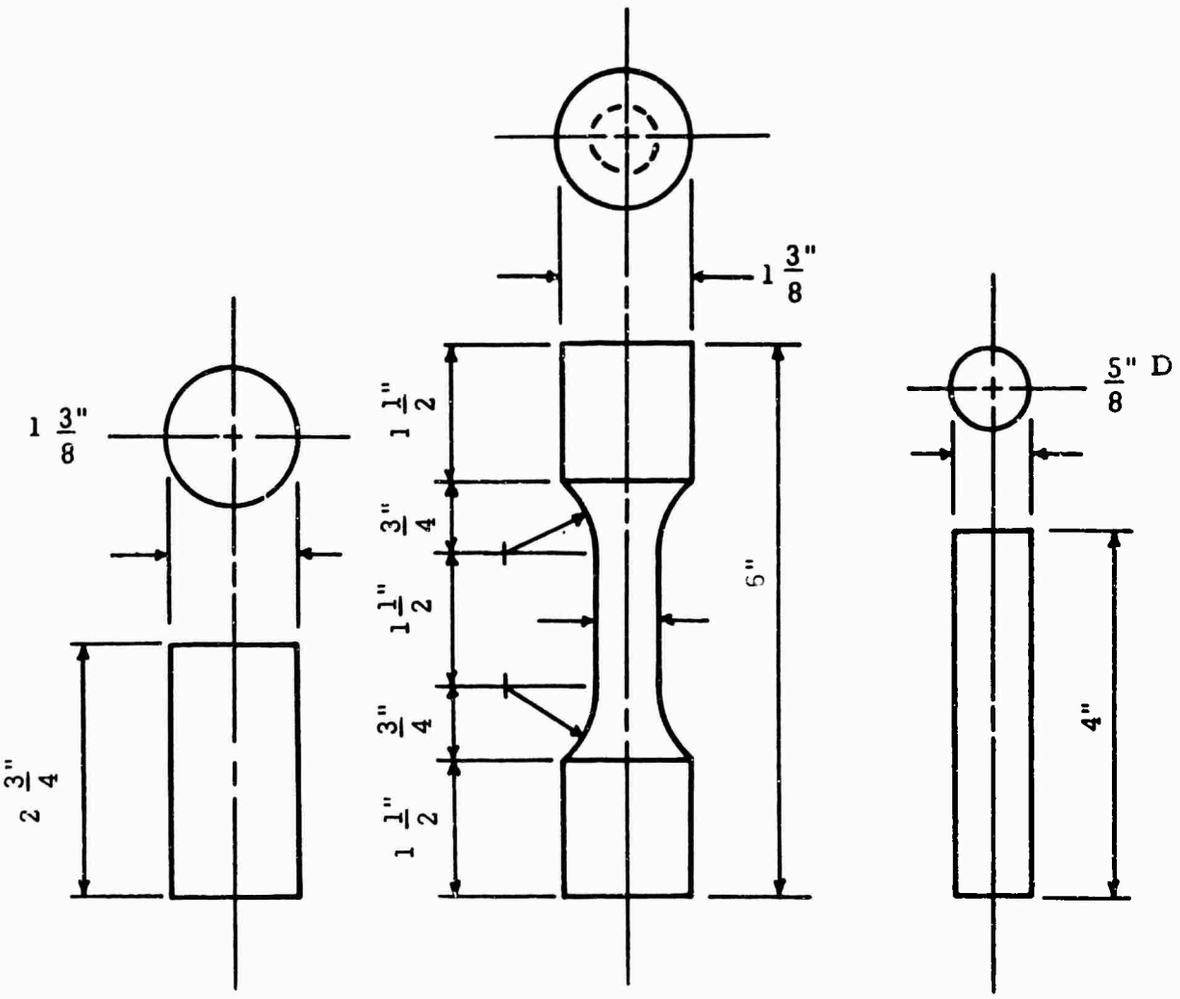

Fig. 5. Details of the Test Specimens.

Easy removal is due to the film of water formed between the casting and the oiled surface of the mold by sweating. After removal, the specimens were cured at room temperature for two weeks before testing.

2.2 Compression Specimens

Three types of specimens were tested: compression, tension, and dynamic (Figs. 2, 3, 4, & 5). The compression specimens (Figs. 4 & 5a) were made by cutting 10 inch cylindrical castings of diameter 1 3/8" into sections of height-diameter ratio equal to 2. Thus, three specimens could be obtained from one casting. A circular section was used because it is preferred over other shapes for uniform stressing in compression[14]. The selection of the ratio of length to diameter of 2 was made to conform with the standard test cylinder of concrete and other brittle materials[14].

2.3 Tension Specimens

The tension specimens (Figs. 3 & 5b) were machined from 6" cylindrical castings of diameter 1 3/8" with the aid of a soil trimmer and lathing tools (Fig. 2).

The large diameter of the ends was necessary in order to avoid failure due to combined axial and grip stresses. The transition from end to reduced section was made by an adequate fillet in order to reduce the stress concentration caused by the abrupt change in section. The specimen was made symmetrical about the longitudinal axis throughout its length in order to avoid bending stresses during application of load.

2.4 Dynamic Specimens

A cylindrical bar was chosen as the dynamic specimen (Fig. 5c) in these and other tests [8,9,10] to study the phenomenon of scabbing because of simplicity in experiments and theoretical anlaysis. Specimens were made by cutting 5/8" diameter cylindrical castings into 4" lengths. The bar dimensions are controlled by several factors. These are: the diameter must be small as compared with the length of the pulse to obtain a close approximation to a uniform stress across the bar. Its diameter must be sufficiently thick to prevent fracture while handling.

The bar length should be longer than half the length of the pulse, but not so long as to cause appreciable dispersion of the pulse during propagation.

Chapter III

STATIC TESTING

Tests were first carried out on compression specimens of different consistencies. The blending time was varied to determine the optimum value at which the mix would have maximum compressive strength. Using the above optimum blending time, tension specimens were made of different consistencies. After obtaining the ultimate tensile strength for each mix, dynamic specimens were cast using only the mix with the highest value of ultimate compressive to tensile strength ratio.

3.1 Compression Test

The compression cylinders were tested to ultimate load in a hydraulic testing machine.

The top and bottom of each cylinder were lubricated to prevent frictional restraint between the surfaces of the cylinder and heads of the testing machine. Care was exercised to obtain accurate centering and alignment of specimen and bearing plates in the testing machine. While the head of the machine was being lowered to contact with a spherical bearing block, the block was rotated slightly by tapping with a small hammer to place the block in a horizontal plane and facilitate the seating of the block. The rate of loading in compression and tension was held quite small and relatively constant at about 10 psi per second. Figure 8 shows some typical compression failures.

3.2 Tension Tests

The tension specimens were tested to ultimate load by dead weights. Before testing, each end of the specimen was covered with a layer of soft paper and clamped into a split section of aluminum tubing (Figs. 6 & 7). About one inch of the tubing extended beyond the ends of the specimen through which steel pins were inserted. The load was applied to knife-edge hooks which rested at the mid-point of the pins.

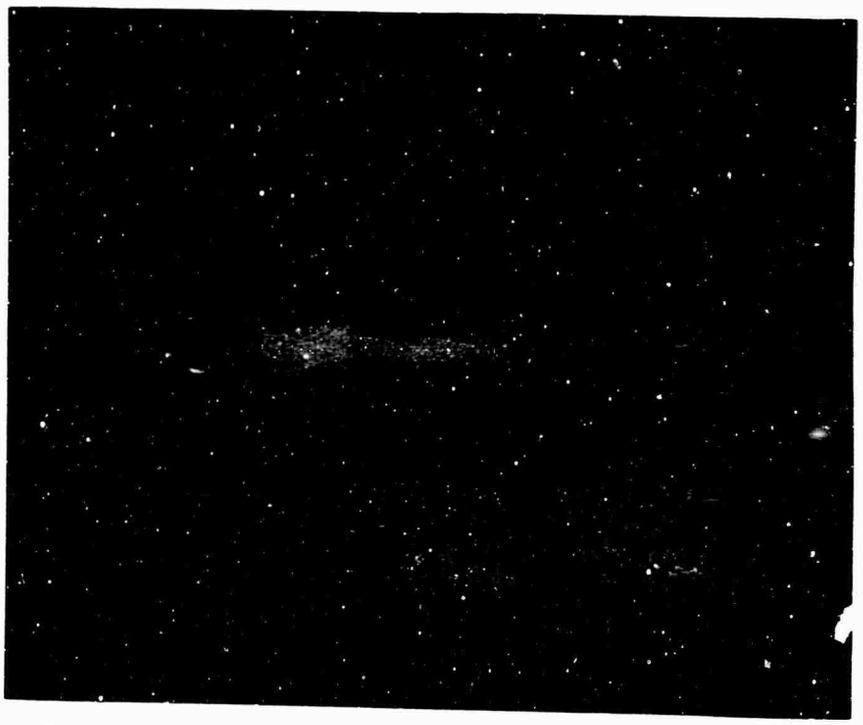

Fig. 6. Photograph of Static Tension Test Assembly.

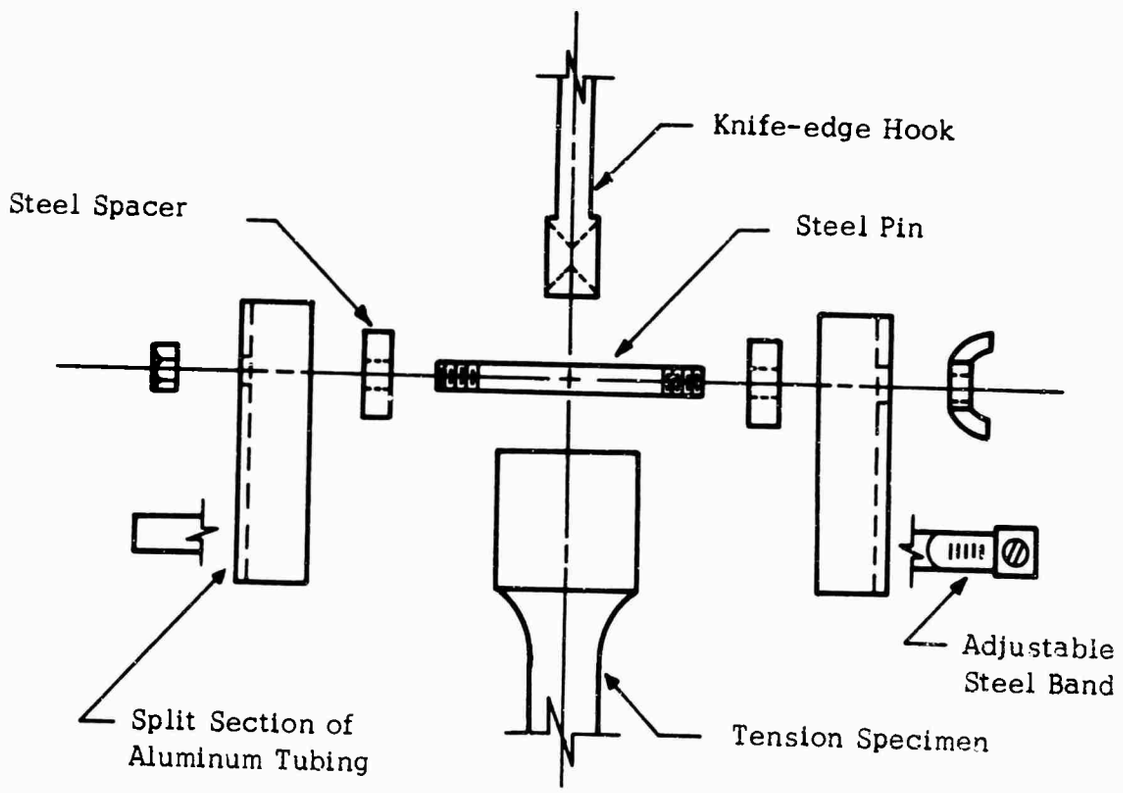

Fig. 7. Details of Tension Test Assembly

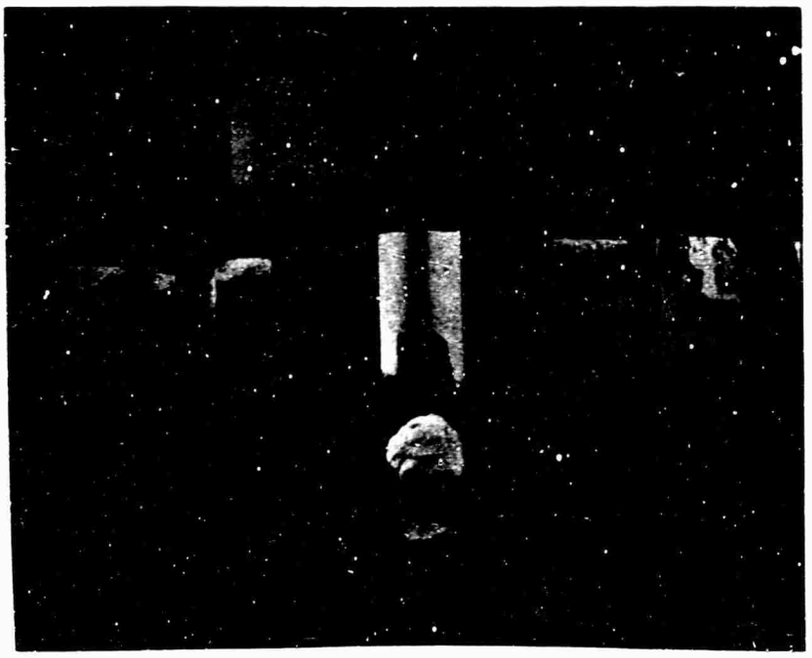

Fig. 8. Typical Static Compression Failures.

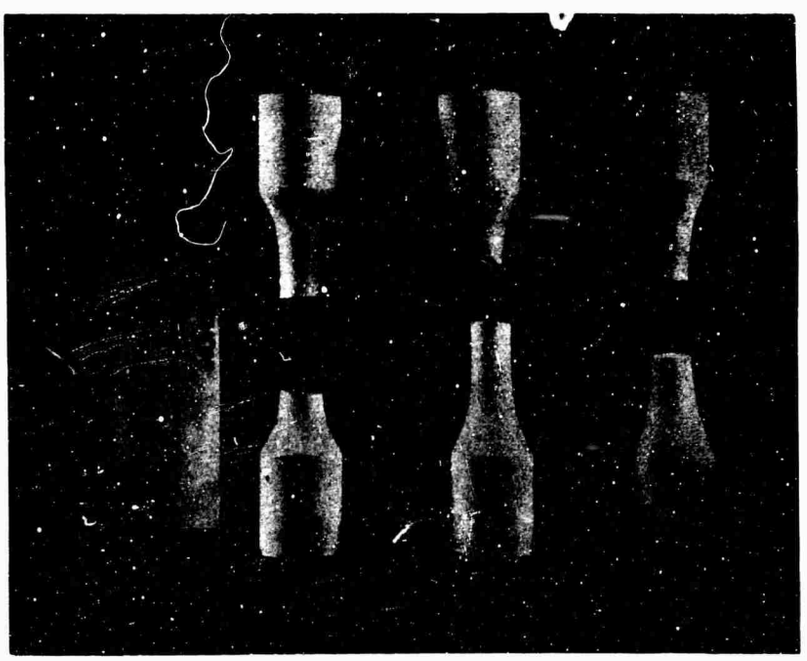

Fig. 9. Typical Static Tension Failures.

This type of gripping device was used to prevent possible bending stresses in the specimen while applying the load. Figure 9 shows some fractured tensile test specimens.

3.3 Results of Static Tests

Table I

Consistency*	Optimum Blending Time (mins)	Ultimate Compressive Strength** S_C (psi)	Ultimate Tensile Strength** S_T (psi)	$\frac{S_C}{S_T}$
65	1	2410	500	4.8
70	3	1670	410	4.1
80	6	1340	350	3.8
90	9	1120	310	3.6
100	12	990	290	3.4

* Parts water per 100 parts plaster by weight
** Determined for specimens prepared with optimum blending time

Several mixes of different consistencies ranging from 65 to 100 were tested statically. An attempt was made to test a mix of consistency equal to 60 but the mix became so stiff that casting was very difficult to accomplish and also the vacuum process explained earlier (Sec. 2.1) had little effect upon removal of entrapped air.

The results of tests to determine the optimum blending time of several mixes are shown in Figure 10. This figure points out the need to control the blending time of each plaster of Paris mix in order to reproduce as nearly as possible the same properties from one casting to another. Figures 11 and 12 show the effect of water content on the ultimate compressive strength and ultimate tensile strength respectively. Both the compressive and tensile strength properties increased with decreasing amounts of water used in the mix.

As explained earlier (Sec. 1.3) the usefulness of plaster of Paris as a dynamic testing material, for studies like those of scabbing, is directly related to its compressive to tensile strength ratio, the higher this value, the better. From Figure 13 it is seen that this ratio increases with decreasing amounts of water used in the mix. It was found that the best mix to be used for dynamic models is one of a consistency equal to 65 parts water per 100 parts plaster because it is easy to mix, remove entrapped air, cast, and has an average ultimate compressive to average ultimate tensile strength ratio equal to about five.

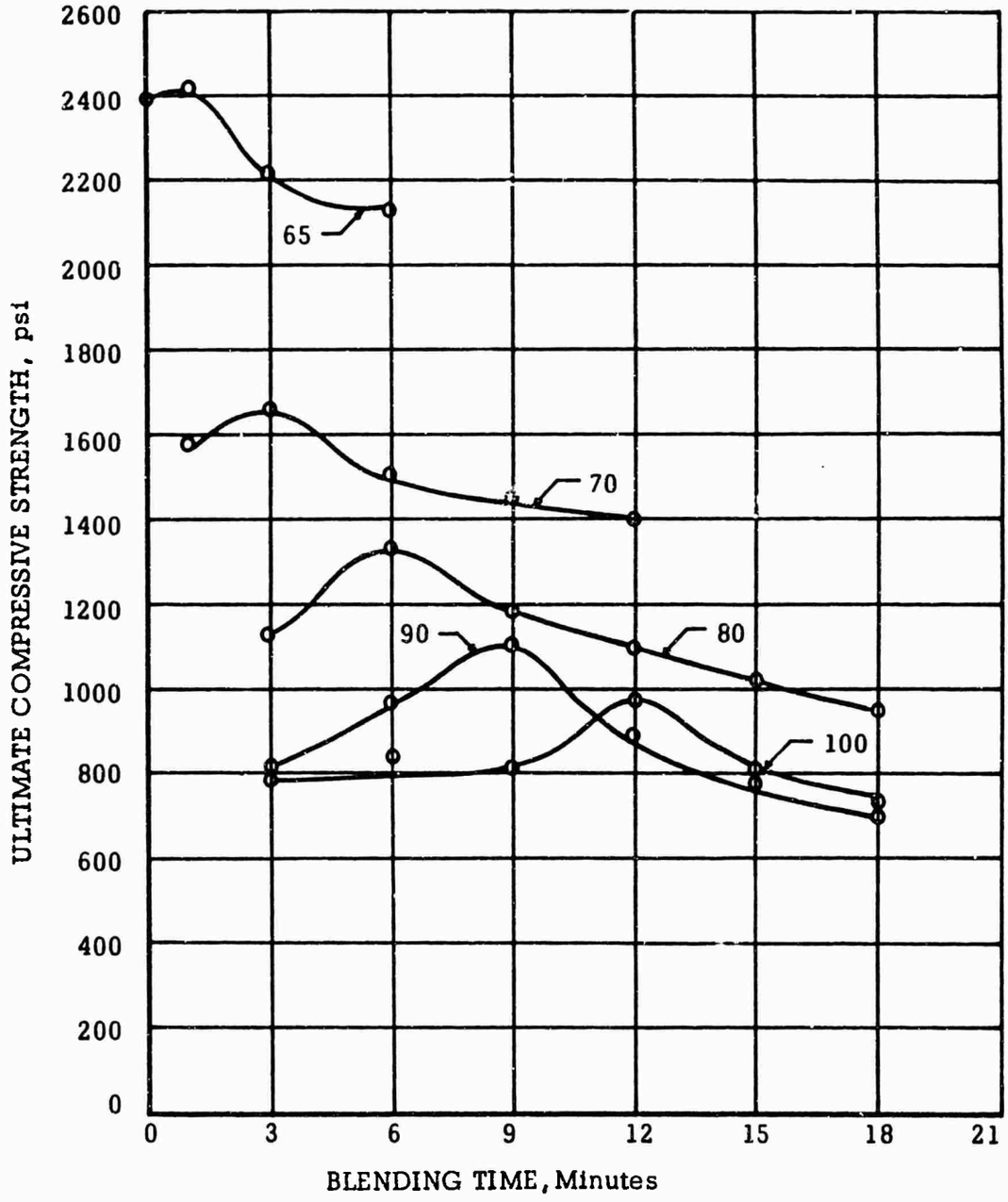

Fig. 10. Ultimate Compressive Strength vs. Blending Time for Consistencies of 65, 70, 80, 90, and 100.

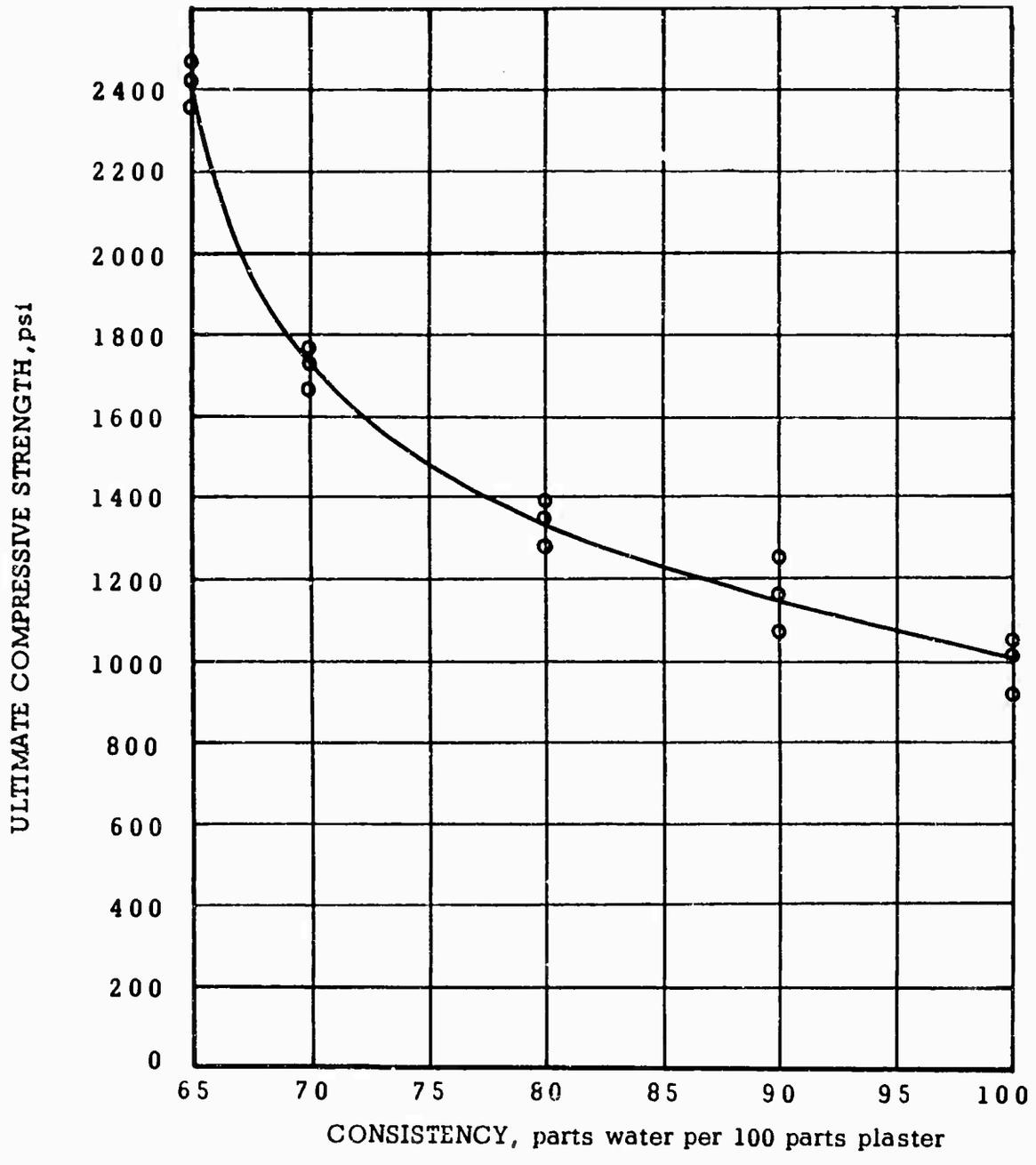

Fig. 11. Ultimate Compressive Strength vs. Consistency.

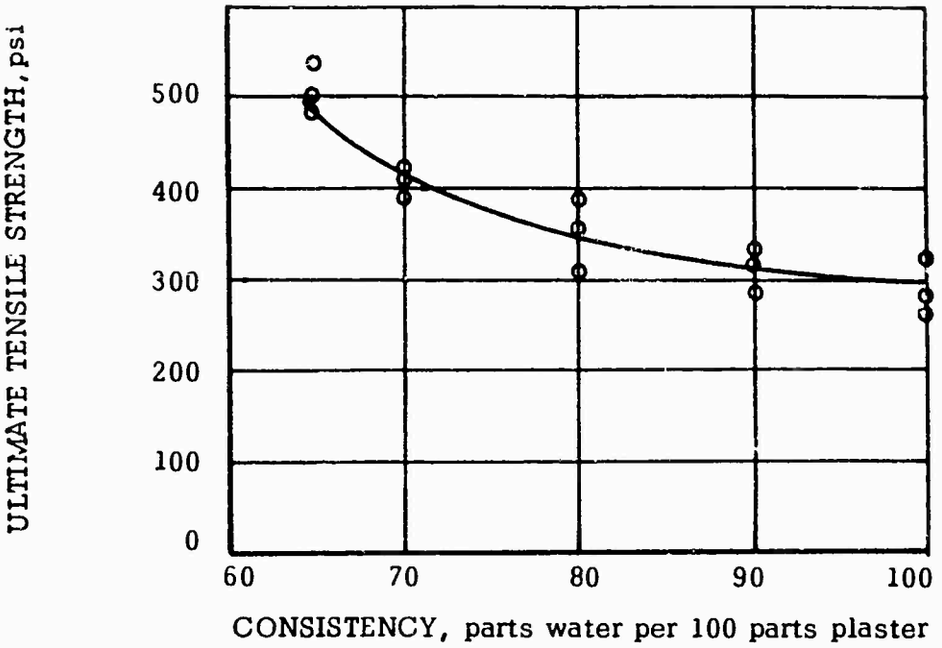

Fig. 12. Ultimate Tensile Strength vs. Consistency.

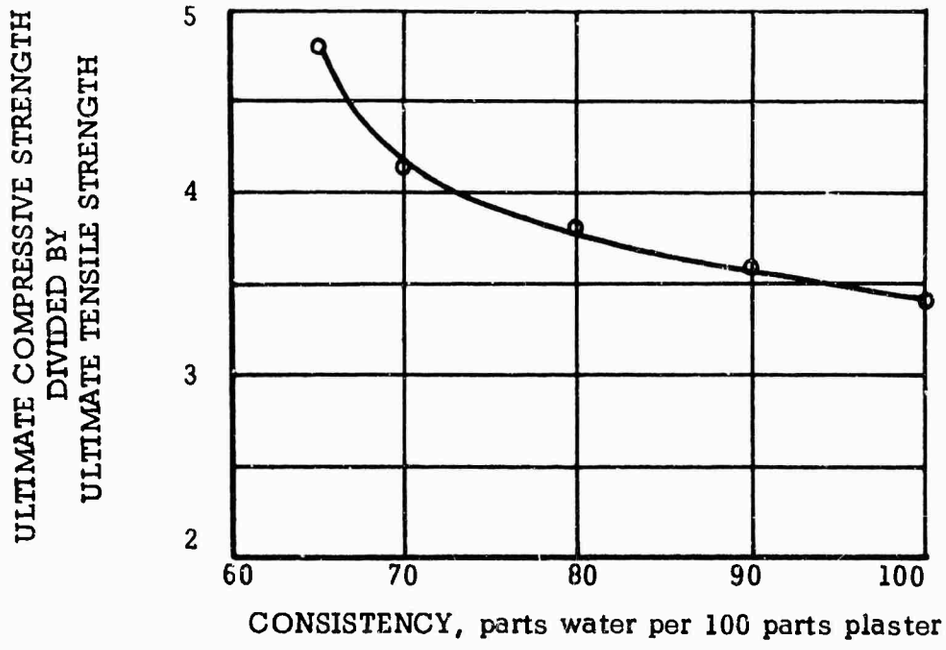

Fig. 13. Ultimate Mean Compressive Strength Divided by Ultimate Mean Tensile Strength vs. Consistency.

Chapter IV

DYNAMIC TESTING

4.1 Introduction

Dynamic tests were carried out on plaster of Paris bars to determine its dynamic modulus of elasticity and dynamic tensile strength. The mix used in these tests was one of a consistency equal to 65 parts water per 100 parts plaster by weight. Since this is the most desirable mix to be used in experimental studies of scabbing, other mixes were not tested. A reverse approach to the intercept method (to be discussed in section 4.3) was used to determine the dynamic tensile strength of plaster bars.

A theoretical and experimental study of pressure pulse shapes produced by longitudinal impact of a pellet on a bar was also carried out to determine under what conditions the most desirable pulse shape is produced for use in dynamic testing of a brittle material such as

plaster of Paris. It is considered a significant part of the thesis, however, because of its distinctly different character it is presented as a major Appendix. This also helps maintain the continuity of presentation of the plaster of Paris properties.

4.2 Determination of the Wave Velocity in Plaster of Paris and the Dynamic Modulus of Elasticity

The wave velocity in plaster of Paris was determined by mounting a type C-11 SR4 strain gage 5 inches from one end of a 10 inch plaster bar. The output of the gage was connected to a Tektronix type-E preamplifier. One end of the bar was impacted with a pellet and the resulting oscillogram shown in (Fig. 14) was to determine the time required for the pulse to travel twice the distance from the gage to the free end of the bar. The first peak on the oscillogram represents the peak pressure of the compressive pulse as it passed the gage, and the second peak represents the peak pressure of the tensile pulse as it passed the gage after being reflected from the free end. Therefore, the time required for the pulse to travel 10 inches is 50×10^{-6} sec/cm x 1.92 cm = 9.6×10^{-5} sec

and the wave velocity in the plaster of Paris bar is $10 \text{ in}/9.6 \times 10^{-5} \text{ sec} = 10.42 \times 10^{4} \text{ in/sec}$. The mass density was determined experimentally and found to be 1.08×10^{-4} #-sec^2-in^{-4}.

Using the relation $c = \sqrt{\frac{E}{\rho}}$, where c is the wave velocity, E is the modulus of elasticity, and ρ is the mass density, the dynamic Young's modulus, E_D, of plaster of Paris was found to be 1.17×10^{6} psi.

4.3 Determination of the Dynamic Tensile Strength

When a sudden compressive pressure of high intensity is applied to one end of a bar, a compressive pulse travels through the bar from the point of application. When this pulse strikes on the free boundary of the other end, it is reflected back into the bar as a tensile pulse propagating in the reverse direction. On interaction of the compressive and tensile pulse, tensile stresses will result and if the material of the bar is weaker in tension than in compression, a fracture or fractures may occur. This phenomenon is referred to as scabbing and the piece which breaks free is called a scab.

50 Microseconds Per Centimeter

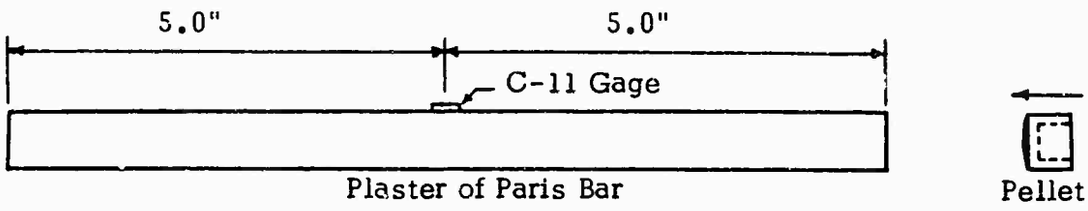

Fig. 14. Determination of the Wave Velocity in a Plaster of Paris Bar.

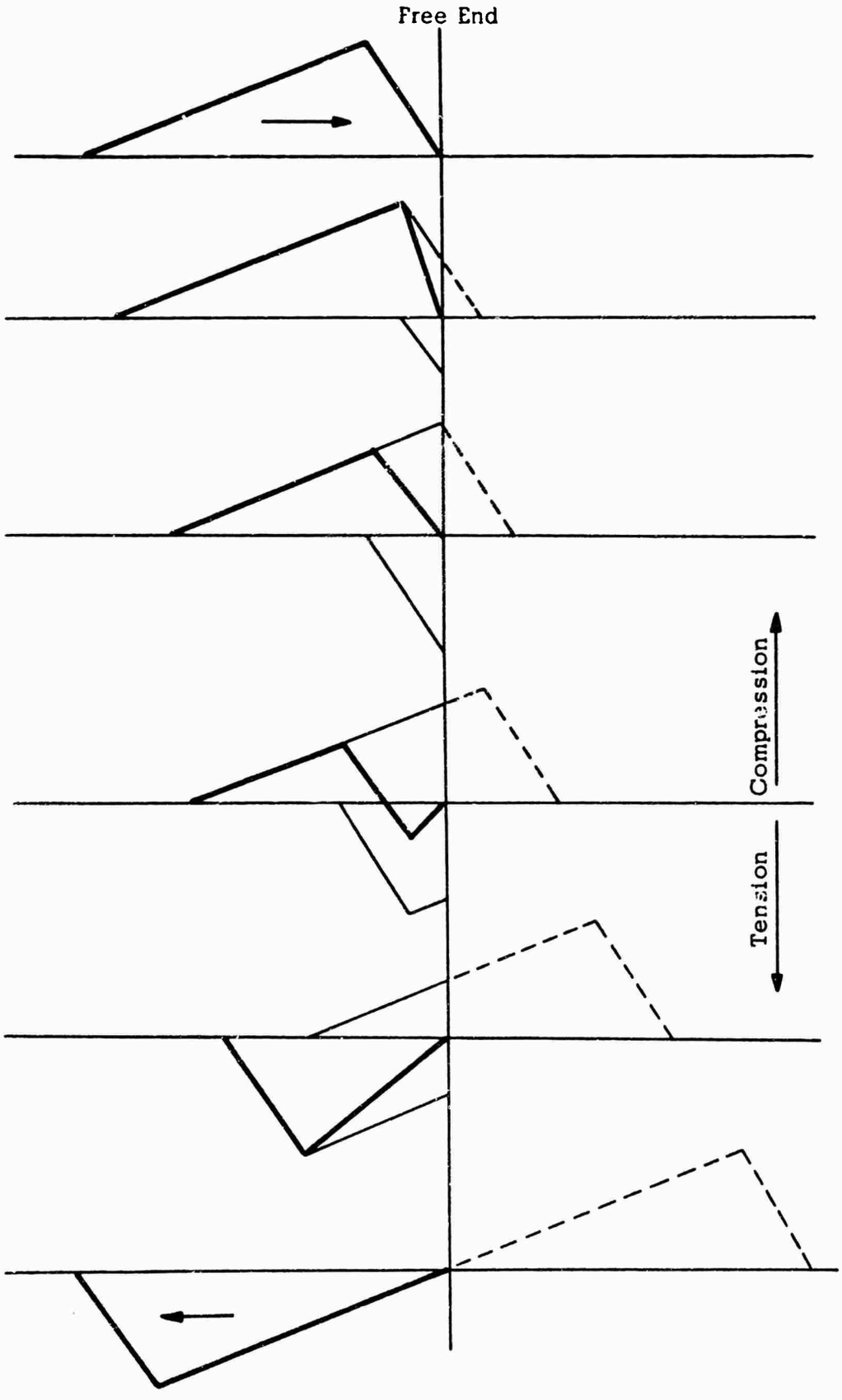

Fig. 15. Reflection of a Compression Pulse at a Free Boundary.

Figure 15 shows the reflection of a triangular compressive pulse at the free boundary of a bar. In order for the stress at the free boundary to be equal to zero, the pulse must reflect with the same magnitude and the opposite sign as the compressive pulse. If the resultant tensile stress becomes larger than the fracture stress of the material, a scab will be formed.

Kumar and Davids[7] suggested the intercept method for the determination of scab lengths formed in a bar or plate due to a strong pressure pulse with a steep front when the shape of the pulse is known. The length of the first scab is obtained by first marking off an intercept (Fig. 16) of length equal to the dynamic tensile strength of the material, S_T, on a vertical line through the point of maximum pressure, P_m. This intercept is projected horizontally to intercept the fall portion of the curve and then projected vertically down on the horizontal abscissa.

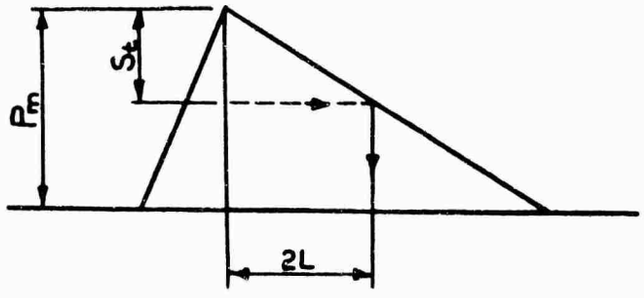

Fig. 16. The Length of the First Scab Determined by Intercept Method.

The length L gives the size of scab formed due to the assumed pressure pulse shape.

Scabbing in materials having a tensile strength less than its compressive strength is a very important phenomenon. It is used in this study as a means of determining the dynamic tensile strengtn of plaster of Paris to be discussed next.

The reverse approach to the intercept method was used to determine S_T when the pulse shape and scab length were obtained experimentally. A distance A-B (Fig. 17) of twice the scab length was marked off on the abscissa, starting from the vertical line through P_m, and projected vertically up an amount X until point B intercepted the curve. Then the vertical distance, X, was subtracted from P_m to determine the dynamic tensile strength, S_T, of plaster of Paris along the plane of fracture. For example, (Fig. 17) shows a pressure pulse which produced a scab length of 1.85 inches and the determined value of S_T. Table I shows the values of the dynamic tensile strength of 5/8" diameter plaster of Paris bars. The average value of eight tests was found to be 1620 psi.

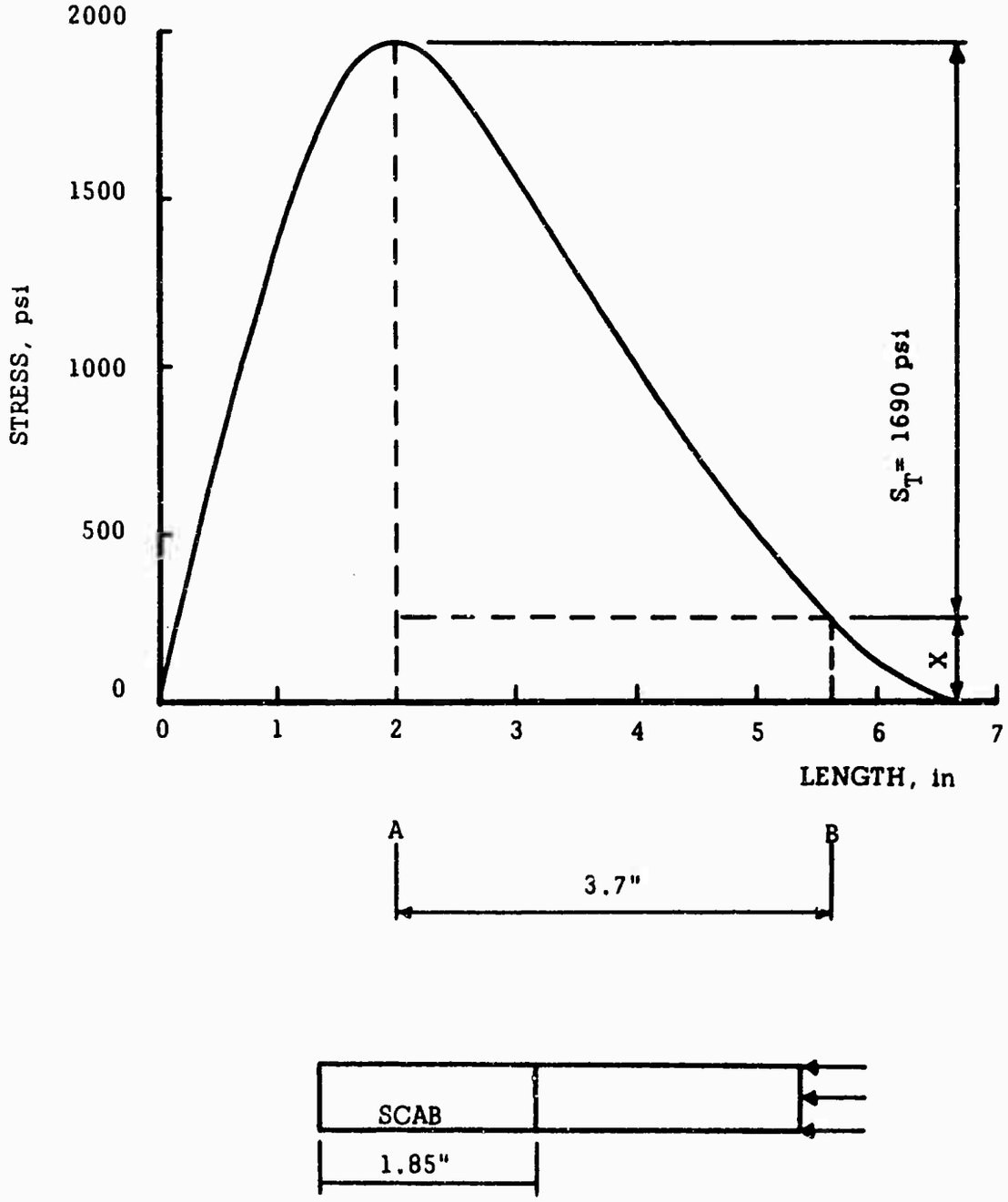

Fig. 17. The Dynamic Tensile Strength Determined by the Reverse Approach to the Intercept Method.

Table II

Dynamic Tensile Strength Values
Of 5/8" Diameter Plaster Bars

Test No.	Pellet Velocity ft/sec	Scab Length in	Dynamic Strength psi
5-A	23.7	1.70	1500
5-B	22.8	1.95	1580
5-C	23.2	1.90	1560
5-D	23.8	2.45	1820
5-E	24.7	1.85	1690
5-F	No Record	2.80	———
5-G	23.2	1.90	1560
5-H	23.8	2.00	1670
5-I	23.8	1.75	1550
5-J	24.5	1.90	1670

Average Dynamic Tensile Strength 1620

Chapter V

CLOSURE

The problem under investigation in this thesis was to assess the feasibility of using plaster of Paris as a modelling material. The general nature and significance of past experiments using plaster of Paris as a model material were discussed briefly and the reasons for using plaster models were pointed out. A schedule for procuring a relatively consistent homogeneous model was introduced and some of the mechanical and physical properties of plaster of Paris were determined. These are,the effect of water ratio and blending time on the static compressive strength, the effect of water ratio on the static tensile strength, and the dynamic tensile strength of the most desirable mix to be used in experimental studies of scabbing.

Some suggestions for further investigation on lines of work presented in this thesis are given as follows:

1. Determine the dynamic compressive strength of the plaster. It may be possible to determine this property by impacting a plaster bar which is fixed at one end and free at the other. Upon impacting the free end, a compressive wave will travel along the bar toward the fixed end. Upon reaching the fixed end of the bar, the compressive wave will be reflected such that the compressive stress at this end will be suddenly increased by a factor of two. Thus it should be possible to determine the dynamic compressive strength by impacting the free end of the bar with increasing impact velocities until a compressive failure occurs at the fixed end.

2. Determine the fracture strength of plaster at various impact velocities. An increase in the impact velocity increases the rate at which the bar is strained with respect to time. Thus by changing the impact velocity, it should be possible to determine the behavior of the fracture strength at various strain rates.

3. Study the damping characteristics of plaster. This may be accomplished by observing the change in pulse shape with respect to time as it propagates along a

plaster bar. Such information is needed to check the assumption that the pulse shape remained unchanged during the dynamic tensile tests.

4. Develop a method by which strain records can be obtained directly from the plaster of Paris bars and a method of triggering the oscilloscope beam before the pressure pulse reaches the measuring gages.

From this study made on plaster of Paris several conclusions can be made. These are:

1. Blending time effects the ultimate strength of the plaster and must be held constant in order to produce the same properties from one casting to another.

2. Application of vibration and vacuum during mixing of the plaster improves the homogeneity of the mix by removing entrapped air.

3. The ultimate compressive and tensile strength of plaster of Paris increases with decreasing amounts of water.

4. The ratio of the ultimate compressive to tensile strength increases with decreasing amounts of water used in the mix.

5. The most desirable mix for dynamic model tests is one of 65 parts water per 100 parts plaster of Paris by

weight. This mix is easily cast and has an ultimate compressive to tensile strength ratio of about five.

6. The reverse approach to the intercept method of determining scab lengths in bars caused by a known pressure pulse was successfully used to determine the dynamic tensile strength of plaster of Paris. This method could also be used to determine the dynamic tensile strength of other brittle materials.

For determining the conditions in which the most suitable pressure pulse could be produced for generating scabs in a rod by longitudinal impact of a pellet, a theoretical and experimental study has been carried out in the appendix of this thesis. The nonlinear differential equation for the pulse shape obtained by utilization of the Hertz Principle was solved numerically by using the Kutta-Simpson one-third rule. The theoretical and experimental pressure pulse shapes for two impact velocities agreed quite well with each other indicating that the Hertz Principle applied reasonably well for impedance mismatch situations like the present and even in the extreme case where the period of the lowest natural mode of one of the impacting bodies is comparable to the duration of impact.

APPENDIX

INVESTIGATION OF PRESSURE PULSE SHAPES PRODUCED BY LONGITUDINAL PELLET-BAR IMPACT

A theoretical and experimental study of pressure pulse shapes produced by longitudinal impact of a pellet on a bar was carried out to determine under what conditions the most desirable pulse shape (discussed later) could be obtained for use in dynamic testing of a brittle material such as plaster of Paris. This study also presented a good opportunity to investigate several recommendations of further study made by Jones[9] and Leu[10] in their studies of the scabbing phenomenon in bars.

Theoretical Investigation

The pressure pulse shape produced by longitudinal impact of a spherical faced pellet on a flat ended bar

may be approximately obtained by utilization of the Hertz Principle of impact [15]. In this principle the compression at the place of contact is regarded as gradually produced, i.e., the local compression due to impact is regarded as a statical effect. If the Hertz Principle is to hold, it is necessary that the duration of impact be large compared with the period of the lowest mode of vibration of either body in question. Since this principle is restrictive, it may yield inaccurate results under certain conditions. The present investigation was therefore conducted to determine the degree to which it applies to our present problem. Its utilization to determine the pressure pulse shape produced by the longitudinal impact of a spherical faced pellet on the flat end of a bar gives a solution which compares well with experimental measurements as will be seen later.

When two spherical bodies are pressed together, local deformation produces contact over a small surface of circular boundary, called the surface of contact. If the radius of curvature of the pellet face and the end of the bar are large in comparison with the radius of the

boundary of the surface of contact, the relative displacement between two chosen points (one on the pellet and the other on the bar) can be assumed to be the same as one for compression on a semi-infinite body by a sphere of radius R, which is [16]

$$u = \sqrt[3]{\frac{9P^2(b_1 + b_2)^2}{16R}} \qquad (1)$$

where u is the relative displacement between the two points, one on the pellet and the other on the bar,

and $b_1 = \frac{1 - \nu_1^2}{E_1}$ and $b_2 = \frac{1 - \nu_2^2}{E_2}$

where R = radius of curvature of the pellet

P = force between the two bodies

ν_1 = Poisson's ratio of the pellet

ν_2 = Poisson's ratio of the bar

E_1 = Young's modulus of the pellet

E_2 = Young's modulus of the bar.

The two points are chosen at sufficient distances from the point of contact such that deformation at these points

due to the compression at the surface of contact can be neglected in comparison to the maximum deformation.

The equation for the pressure pulse shape is [10,17]

$$\frac{d^2B}{dt^2} = a_1 B^{\frac{1}{2}} \frac{dB}{dt} + \frac{2}{3} a_2 B^{\frac{3}{2}} \qquad (2)$$

in which $B = P^{\frac{2}{3}}$, t = time ,

$$a_1 = - \frac{3}{2A \sqrt[3]{\frac{9(b_1 + b_2)^2}{16R}} \sqrt[2]{E_2 \rho_2}} ,$$

and

$$a_2 = - \frac{3}{2m_1 \sqrt[3]{\frac{9(b_1 + b_2)^2}{16R}}} ,$$

where, A = cross-sectional area of the bar

ρ_2 = density of the bar

m_1 = mass of the pellet

The two initial conditions for equation (2) are:

(1) $P = 0$ at $t = 0$ $\qquad$ $B = 0$ at $t = 0$

(2) $\frac{du}{dt} = V$ at $t = 0$,

where V is the impact velocity of the pellet and the other parameters are the same as above.

The initial condition $\frac{du}{dt} = V$ at $t = 0$ is expressed from equation (1) in terms of $\frac{dB}{dt}$ as follows:

$$\frac{du}{dt} = \frac{2}{3} K P^{-\frac{1}{3}} \frac{dP}{dt} = V$$

where $K = \sqrt[3]{\frac{9(b_1 + b_2)^2}{16R}}$

Since $P = B^{\frac{2}{3}}$,

$$\frac{dP}{dt} = \frac{3}{2} B^{\frac{1}{3}} \frac{dB}{dt}$$

or $$P^{-\frac{1}{3}} \frac{dP}{dt} = \frac{3}{2} \frac{dB}{dt}$$

Therefore $$\frac{du}{dt} = K \frac{dB}{dt} = V$$

Hence the two initial conditions for equation (2) are:

(1) $B = 0$ at $t = 0$

(2) $\frac{dB}{dt} = \frac{V}{K}$ at $t = 0$

Equation (2) is put in the form of two simultaneous equations of the first order by introducing a new variable $Z = \frac{dB}{dt}$. We now have

$$\frac{dB}{dt} = Z = f(t, B, Z) \tag{3}$$

and $$\frac{dZ}{dt} = a_1 B^{\frac{1}{3}} Z + \frac{2}{3} a_2 B^{\frac{2}{3}} = g(t, B, Z) \tag{4}$$

Leu obtained a second approximation solution of the above equation by breaking it into two linear equations and using Picard's method of successive approximations. This solution did not agree with his experimental results too well. For this reason the author solved the equation numerically. The calculations were done with the aid of the I.L.M. 7070 digital computer at Duke University.

The above two equations are in the form

$$\frac{dy_i}{dt} = y'_i = f_i\left[t, y_1(t), y_2(t)\right] \quad \text{for } i = 1,2$$

with the initial conditions

$$y_1(0) \equiv f(0) \equiv Z_0 = \frac{V}{K} \quad \text{where } (Z_0 = Z \text{ at } t = 0)$$

$$y_2(0) \equiv g(0) \equiv B_0 = 0 \quad \text{where } (B_0 = B \text{ at } t = 0)$$

The numerical solution of the above equations satisfying the initial conditions involves determination of $y_1(0 + \Delta t)$ and $y_2(0 + \Delta t)$ corresponding to an increment Δt of the independent variable t. This is usually accomplished by expanding the two functions $y_1(t)$ and $y_2(t)$ in a Taylor's series form and approximating it with two, three, or four finite terms depending on the accuracy desired. The coefficients assigned to each of these finite terms can be determined in many many ways, according to which dozens of rules have been given by

different workers. One of the standard methods using this approach is the Runge-Kutta Method [18]. Here we will use the fourth order approximation [18] of this method, according to which we have the following formulas for calculating the changes ΔB and ΔZ in equations (3) and (4) for the first increment Δt of the independent variable t.

$$\Delta B = \frac{1}{6}(k_1 + 2k_2 + 2k_3 + k_4)$$
$$\Delta Z = \frac{1}{6}(l_1 + 2l_2 + 2l_3 + l_4) \qquad (5)$$

in which (for $\Delta t = h$)

$$\begin{aligned}
k_1 &= f(t_o, B_o, Z_o)h \\
l_1 &= g(t_o, B_o, Z_o)h \\
k_2 &= f(t_o + \tfrac{1}{2}h, B_o + \tfrac{1}{2}k_1, Z_o + \tfrac{1}{2}l_1)h \\
l_2 &= g(t_o + \tfrac{1}{2}h, B_o + \tfrac{1}{2}k_1, Z_o + \tfrac{1}{2}l_1)h \\
k_3 &= f(t_o + \tfrac{1}{2}h, B_o + \tfrac{1}{2}k_2, Z_o + \tfrac{1}{2}l_2)h \\
l_3 &= g(t_o + \tfrac{1}{2}h, B_o + \tfrac{1}{2}k_2, Z_o + \tfrac{1}{2}l_2)h \\
k_4 &= f(t_o + h, B_o + k_3, Z_o + l_3)h \\
l_4 &= g(t_o + h, B_o + k_3, Z_o + l_3)h
\end{aligned} \qquad (6)$$

where t_o, B_o, and Z_o are the initial values. The values of t, B, and Z for the first increment h are now

$$\begin{aligned}
t_1 &= t_o + h \\
B_1 &= B_o + \Delta Z \\
Z_1 &= Z_o + \Delta Z
\end{aligned}$$

The values of t, B, and Z for the second increment are computed by the same formulas (5) and (6), with (t_o, B_o, Z_o) replaced by (t_1, B_1, Z_1). Thus all intervals are computed in the same manner, using for the initial values the values at the beginning of each interval.

The Runge-Kutta Method was chosen to solve equation (2) because of the following reasons: It is well adopted for computer programming since all intervals are computed in the same manner. This method does not need any special formulas to get the solution started. Also, the inherent error in this method is of the order h^5 as it approximates the Taylor's series out to and including terms in h^4, h being the magnitude of the interval.

The above method was used for numerical determination of pressure pulse shapes and rise times in longitudinal impact of spherical faced pellet with a flat ended bar. This helped us decide the conditions under which a most suitable pressure pulse would be generated for our scabbing experiments.

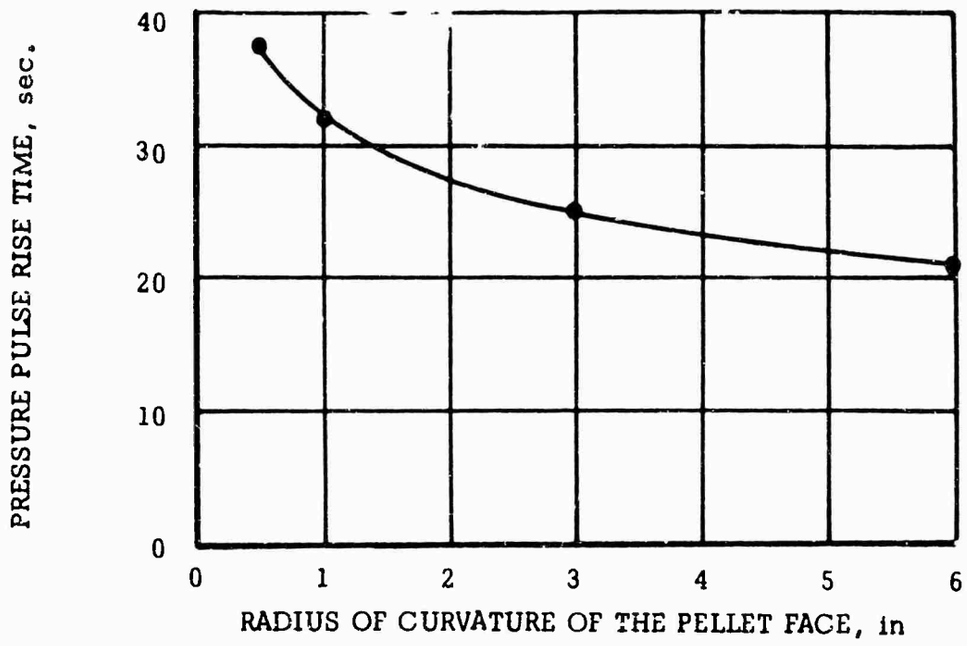

Figure 18. Variation of Rise Time With Radius of Curvature of the Face of the Pellet for V = 30 fps.

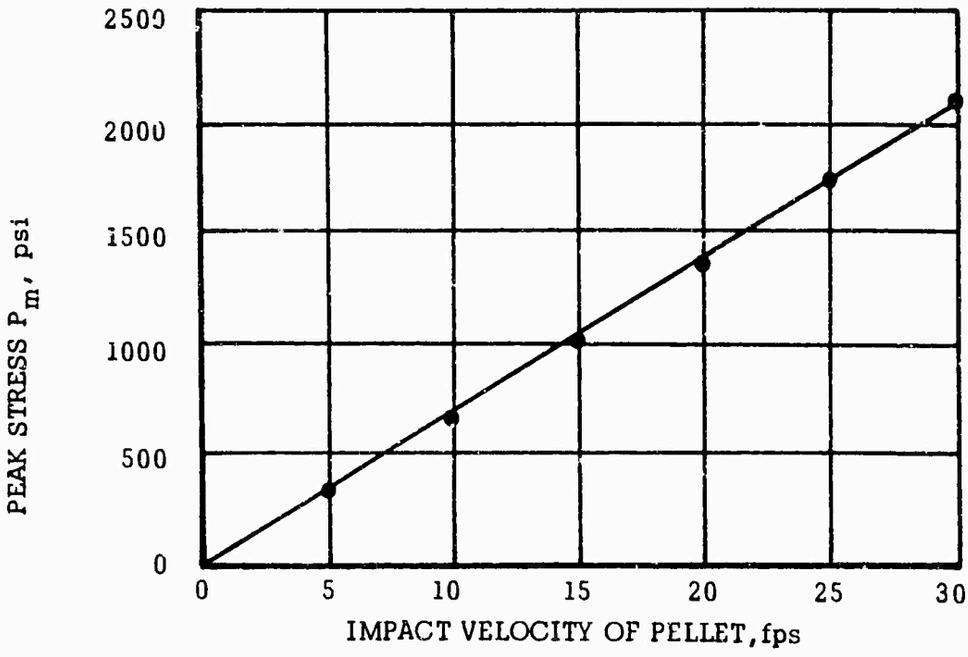

Figure 19. Variation of Peak Stress with Impact Velocity of Pellet for R = 6 in.

The pressure pulse shape desired for scabbing tests is one in which the peak pressure is produced in a short time. The longitudinal impact of two bars with flat ends will produce a pulse in which the rise time, i.e., the time required to obtain maximum pressure upon impact, is smallest [10]. However, this requires instantaneous perfect contact of two flat surfaces at the time of impact which is very difficult to achieve experimentally (because perfect axiality is hard to achieve). If, the pulse is produced by impacting the bar with a pellet in which the impact end is spherical in shape, the chance of eccentric impact will be reduced. Figure 18 shows the theoretical variation of rise time with respect to the radius of curvature of the pellet at an impact velocity of 30 fps. From this graph a pellet face radius of 6 inches was selected for the tests because it could be machined reliably and should produce a pulse with a relatively small rise time. An impact velocity of 25 fps was selected with the aid of Figure 19 which shows the theoretical variation of maximum pressure with respect to impact velocity. This velocity was chosen to insure that at least one scab would be formed. A comparison of the theoretical and measured pressure pulse shapes for longitudinal impact of a steel pellet on a lucite bar will be discussed next.

Experimental Investigation

The pressure pulses were produced in the bar by impacting a 10.5 gram steel pellet (5/8" in diameter with a face radius of 6") onto one end of a lucite bar. The pellet was fired through a brass tube of internal diameter slightly larger than that of the pellet, at velocities of 10 to 30 feet per second by a compressed spring. The spring was compressed in varying amounts until the desired velocity for testing was obtained. In previous experiments [9,10] compressed air was used to propel the pellet, but it was found that for the above range more consistent velocities are produced by using a compressed spring. The impact end of the bar was inserted into the tube 1/16" to improve axial alignment of the pellet with the bar. The bar was supported by a longitudinally split section of tubing of the same type used to guide the pellet. This section was axially aligned with the tube and held in

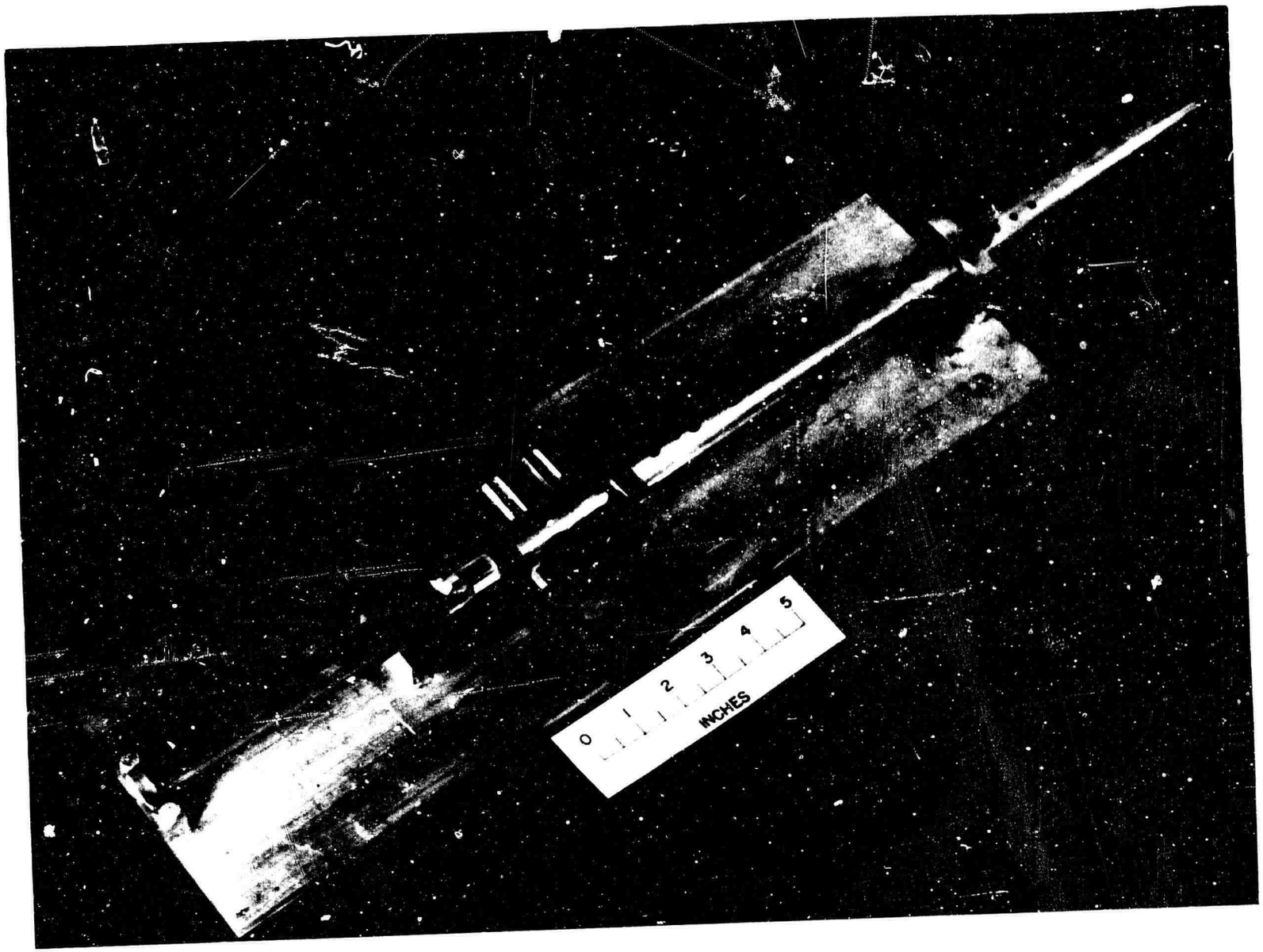

Fig. 20. Photograph of Experimental Setup.

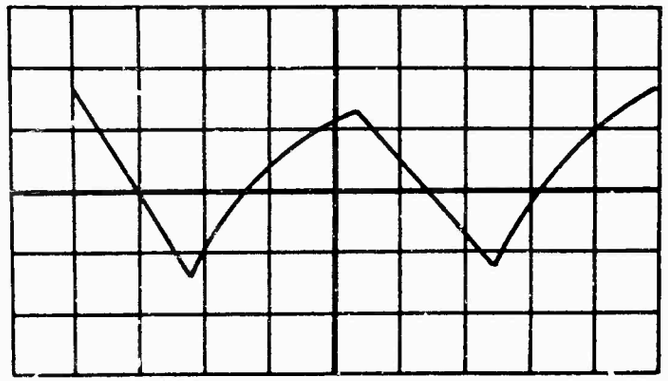

Typical Velocity Record

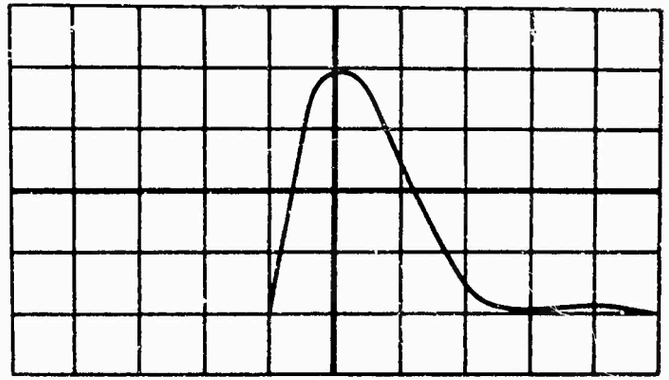

Typical Pulse Record

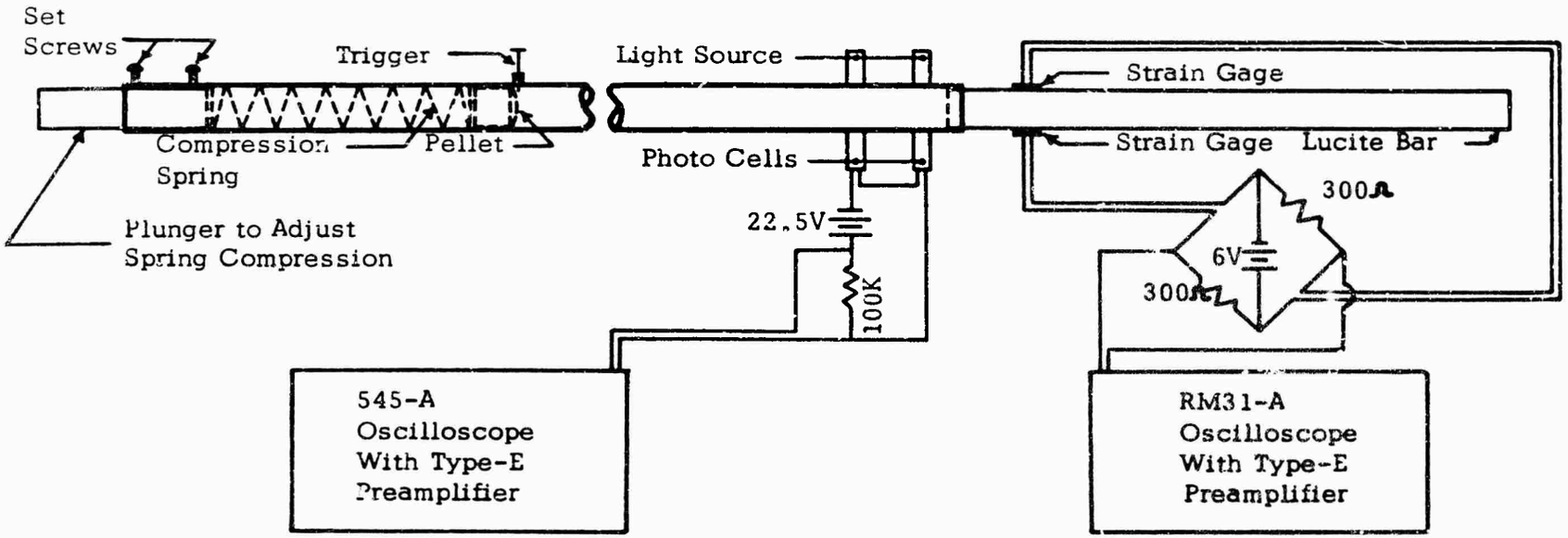

Figure 21. Schematic Diagram of Experimental Setup.

place by brackets. The 6 inch radius of curvature on the pellet face also improved the axiality of impact. This arrangement is shown in the photograph of Figure 20 and in the schematic diagram of Figure 21. For each test two measurements were recorded; one to determine the pellet velocity and the other to determine the pulse shape.

The velocity was calculated by measuring the time interval required by the pellet to traverse a known distance along the tube. The time interval was recorded on a Type 545A-Tektronix oscilloscope with a type-E plug-in-preamplifier. Two photo conductor cells were mounted near the muzzle end of the tube in holes drilled one inch apart. The photo cells were connected in series with a 100K ohm resistor and a 22 1/2 volt battery, and the output across the resistor was connected to the preamplifier as shown in Figure 21. A light source supplied by two 6-volt light bulbs was mounted on the opposite side of the tube from the photo cells. As the pellet moved down the tube and began cutting off the light on the first photo cell, it caused the voltage potential across the resistor to be decreased thereby triggering the oscilloscope time base. When the pellet completely covered the hole, a

maximum potential drop occurred across the resistor which is represented by the first peak on the oscillogram (Figure 21), and upon covering the second hole, a similar maximum potential drop occurred which corresponds to the second peak on the oscillogram. The time required by the pellet to traverse the distance between the photo cells was obtained from the oscillogram by measuring the horizontal distance between the peaks and multiplying by the sweep rate of the oscilloscope beam. With the time and distance being known, the pellet velocity was easily calculated.

The pressure pulse shape was recorded on a type RM31A Tektronix oscilloscope with a type-E plug-in preamplifier. A pair of SR^4 type C-11 strain gages were mounted diametrically opposite to each other and about one inch from the impact end. These gages were connected to opposite sides of the bridge circuit shown in Figure 21 so as to eliminate the effect of flexural strains. This type of arrangement also caused a gain in sensitivity of twice that of a single active gage. The following procedure was used to correlate the vertical deflection on the oscilloscope screen to the strain in the gage.

One C-11 gage was connected to a Baldwin strain indicator and the balanced reading, R_o, was recorded. Then a resistor, R, was shunted across the gage. The bridge was balanced and the second reading, R_1, was recorded. The gage was then connected in the bridge circuit shown in Figure 21 and the same resistor, R, was shunted across the gage. This caused a millivolt deflection, d, on the oscilloscope screen. The conversion factor, K, used to convert the oscilloscope beam deflection to stress in the bar was then obtained from the following relation:

$$K = (R_1 - Ro)\, E_D/2d \quad \text{psi/millivolt deflection.}$$

The factor of two in the denominator was used since there were two active gages. The value of R used was 200,000 ohms which caused an apparent strain, $(R_1 - R_o)$, of 522×10^{-6} in/in in the gage and a deflection d, of 1.1 millivolts on the oscilloscope screen. The dynamic value of Young's modulus, E_D, was determined in a similar manner as described in Section 4.7 and was found to be 8.4×10^5 psi. Thus, as calculated from the above expression, K was found to be equal to 199 psi/millivolt deflection, that is, 1 millivolt deflection on the oscilloscope screen corresponded to 199 psi stress in the bar.

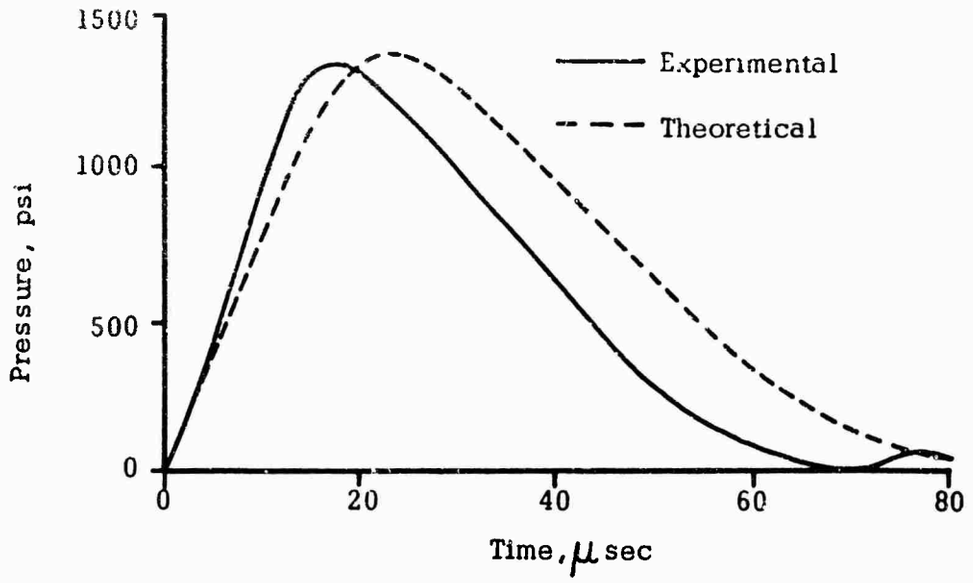

Figure 22. Comparison of Theoretical and Experimental Pressure Pulse Shapes for R = 6 in. and V = 20 fps.

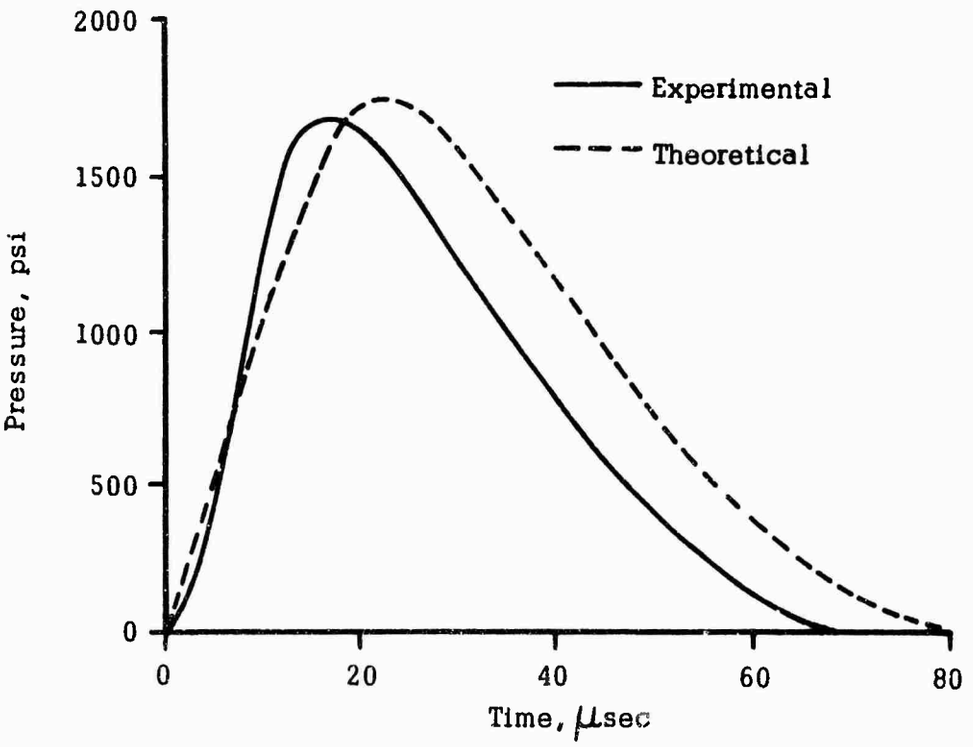

Figure 23. Comparison of Theoretical and Experimental Pressure Pulse Shapes for R = 6 in. and V = 25 fps.

The first series of tests were performed to determine how well the Hertz Principle of longitudinal impact of a pellet on a bar would predict the pressure pulse shape. Since the strains were measured on the surface of the bar, in accordance with Saint-Venant's principle, it was assumed that the compressive force applied at the end of the bar became, as in static loading, uniformly distributed over the cross-section of the bar within a few diameters. The tests were performed using a steel pellet with spherical face of radius 6 inches and impact velocities of 20 and 25 feet per second. For each impact velocity at least ten records were made from which it was found that the velocity and pulse shape measurements were quite reproducible (velocity, pressure and time deviations less than 5%). The representative pulse shapes for the two impact velocities are shown in comparison with the theoretically predicted shapes in Figures 22 and 23. The theoretical and experimental values of peak pressure, rise time, and pulse duration are:

	Velocity = 20 fps		Velocity = 25 fps	
	Theoretical	Experimental	Theoretical	Experimental
Peak pressure-psi	1370	1320	1750	1690
Rise time- μsec	23	17	22	16
Pulse duration- μsec	85	71	84	69

The experimental values of the maximum pressures are within 4% of the theoretical values for both velocities. The significant error in rise time may have been caused by the method used to trigger the oscilloscope beam. Triggering was accomplished internally by the output signal received from the strain gage bridge circuit used to measure the pulse shape. As a result the beam could not start its horizontal sweep until it was deflected a certain amount vertically, thereby, causing the recorded pulse shape to be shifted out of phase with respect to the theoretical curve. Had the beam been triggered just before the pulse reached the measuring gages, this difference in the two pulse shapes may have been reduced. Other factors which may have caused discrepancies between the two curves are:

1. A non-uniform stress distribution over the cross-section.
2. Imperfect spherical face on the pellet (error of 1" in R would change the rise time an order of 1 μsec).
3. The dynamic response of the strain gages.
4. Velocity measurements.

To calculate the dynamic tensile strength of a plaster of Paris bar (as in Section 4.3) it is necessary that the pressure pulse shape producing fracture be known. The use of SR-4 strain gages attached to plaster bars does not indicate the actual strain [9]. Hence, the pressure pulse shape producing fracture must be measured by some alternate method. A method used by previous investigators [9,10] to avoid this difficulty in trying to record the dynamic strains directly from gages mounted on plaster of Paris bars is known as the "lucite strain pickup method". A short lucite bar was attached longitudinally to the plaster bar with a thin film of grease. The strain measurement was done through two SR-4 strain gages attached to the lucite bar. Further it is assumed that if the acoustic impedance of plaster is matched with that of lucite (this can be accomplished within 5-10%) the pressure pulse recorded in the lucite bar represents the pressure pulse transmitted to the plaster bar. In order for an acoustic impedance match to exist, the following relation must hold.[9]

$$\rho_1 c_1 = \rho_2 c_2 ,$$

where ρ_1 and ρ_2 are densities of each material and c_1 and c_2 are the respective longitudinal wave velocities.

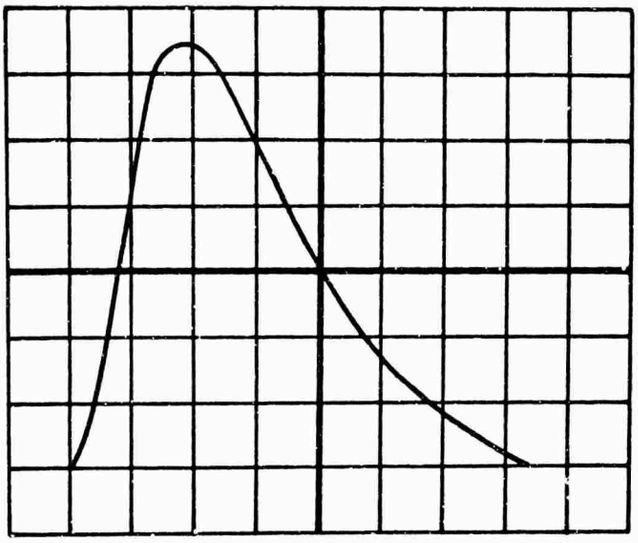

Fig. 24. Pressure Pulse Shape Before Propagation Across the Affixed Ends of Two Bars of Lucite.

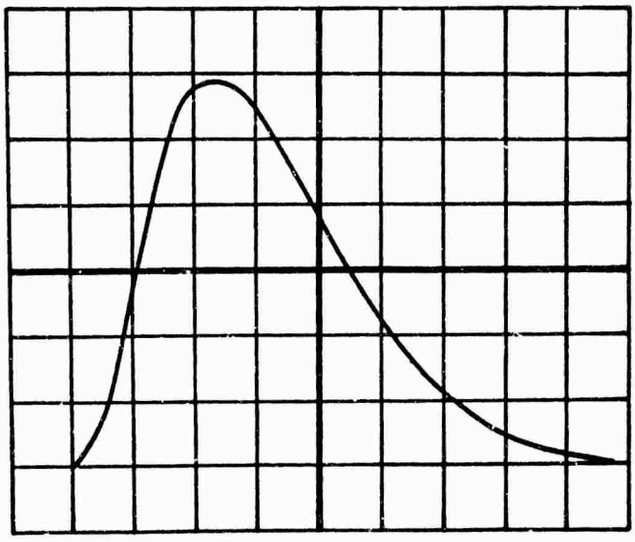

Fig. 25. Pressure Pulse Shape After Propagation Across the Affixed Ends of Two Bars of Lucite.

An experiment was conducted using two cylindrical bars of lucite (exact impedance match) 3 inches long which were attached end to end by grease. Two SR-4 strain gages were affixed to one bar and connected to the bridge circuit shown in Figure 21. The impedance of the two bars was matched, so a pressure pulse should transmit from one to the other without much change in shape. A steel pellet was fired on the bar with gages and the puise recorded (Figure 24). The position of the bars was reversed and the pulse recorded after transmission across the affixed ends (Figure 25). As can be seen from the two oscillograms the pulse has lengthened and decreased in amplitude even though the acoustic impedance of each bar is identical. This distortion of the transmitted pulse is attributed as being due to the imperfect grease bond between the bars. The above procedure was repeated at least ten times and it was found that the results were nearly duplicated for each test.

The wave velocity for plaster of Paris was found to be (Section 4.2) 10.42×10^4 in/sec and its density as 1.08×10^{-4} lb-sec^2-in^{-4}. Therefore, its acoustic

impedance is 11.25 lb-sec-in^{-3}. The wave velocity in a lucite bar was determined by the method used in Section 4.2 and found to be 8.58×10^{4} in/sec and its density as 1.14×10^{-4} lb-sec^{2}-in^{-4}. Therefore, its acoustic impedance is 9.78 lb-sec-in^{-3}. Since the impedance of plaster of Paris and lucite are not the same, the pulse shape dispersion should be more pronounced than that shown in Figures 24 and 25. As a result, the dynamic tensile strength of plaster of Paris bars was not calculated from pressure pulse shapes recorded by the "lucite strain pickup method".

As shown earlier the theoretical and experimental pressure pulse shapes, after maximum pressure is reached, are about the same for a lucite bar. It is this part of the curve that was used to calculate the dynamic tensile strength of a plaster of Paris bar in Section 4.3. Since the theoretical and experimental shapes of the pressure curves after P_{max} are about the same for lucite, it was assumed that this agreement would also exist for plaster of Paris. Using the theoretical pressure pulse, the dynamic tensile strength of plaster of Paris was calculated using the respective velocities and scab lengths from each test. The calculated values are given in Table II.

BIBLIOGRAPHY

1. R.E. Peterson, An Investigation of Stress Concentration by Means of Plaster of Paris Specimens, Mechanical Engineering, Vol. 48, 1926, pp. 1449-452.

2. Fred B. Seely and Richard V. James, Plaster-Model Method of Determining Stress. University of Illinois, Engineering Experimental Station Bulletin, No. 195, 1929, p. 33.

3. Fred B. Seely and Thomas J. Dolan, Stress Concentration at Fillets, Holes, and Keyways as Found by the Plaster-Model Method. University of Illinois, Engineering Experimental Station, Bulletin 276, 1935.

4. W. Trinks and J.H. Hitchcock, Strength of Roll Necks. Transaction ASME, Vol. 55, 1933, RP 55-5, pp. 67-74.

5. N.M. Newmark and Lepper, Tests on Plaster Model Slabs Subjected to Concentrated Loads, University of Illinois, Engineering Experimental Station, Bulletin 313, 1939.

6. R.C. Coates and J.A.N. Lee, Use of Gypsum Plaster as Model Material. Civil Engineering (London), Vol. 52, No. 617, November 1957, pp. 1261-3.

7. S. Kumar and N. Davids, Multiple Scabbing in Materials. J. Franklin Institute, Vol. 263, No. 4, April 1957, pp. 295-302.

8. S. Kumar, Some Futher Studies on Scabbing in Materials. Proceedings of the Fifth Congress on Theoretical and Applied Mechanics, Rookee, December 1959, C36.

9. Alan L. Jones, Studies of Scabbing in Bars and Plates by Plaster Models. M.S. Thesis, Department of Engineering Mechanics, Pennsylvania State University, 1960.

10. Liow-Min Leu, Scabbing and Longitudinal Impact of Bars Using Plaster Models. M.S. Thesis, Department of Civil Engineering, Duke University, 1960.

11. U.S. Gypsum Company, Fundamental Factors in the Use of Pottery Plaster. Ceramic Industry, March 1925.

12. H.C. Fischer, Setting of Gypsum Plaster. American Society Testing Materials, Bulletin No. 192, September 1953, p. 43-7.

13. J.J. Russell and F.A. Blakey, Physical and Mechanical Properties of One Cast Gypsum Plaster, Australian Journal Applied Science, Vol. 7, No. 2, June 1956, p. 176-90.

14. Davis, Troxell, and Wiskocil, The Testing and Inspection of Engineering Materials. McGraw-Hill Book Company, Inc., New York, 1955, pp. 117-127.

15. A.E.H. Love, The Mathematical Theory of Elasticity. Cambridge University Press, 1934.

16. Timoshenko and Goodier, Theory of Elasticity. McGraw-Hill Book Company, Inc., 1951.

17. E.A. Ripperger, The Propagation of Pulse in Cylindrical Bars --- An Experimental Study. Proceedings of the First Midwestern Conference on Solid Mechanics, 1953.

18. Kaiser S. Kunz, Numerical Analysis. McGraw-Hill Book Company, Inc., 1957.